



Agnostic sampling transceiver

ARIJIT MISRA,^{1,2,*}  JANOSCH MEIER,^{1,2} STEFAN PREUSSLER,¹ 
KARANVEER SINGH,¹  AND THOMAS SCHNEIDER¹ 

¹THz-Photonics Group, Institut für Hochfrequenztechnik, Technische Universität Braunschweig,
Schleinitzstraße 22, 38106 Braunschweig, Germany

²Equal contribution

*arijit.misra@ihf.tu-bs.de

Abstract: Increasing demands for data centers, backbone, access, and wireless networks require inventive concepts to transmit and distribute digital or analog signal waveforms. We present a new, extremely simple transceiver concept, fundamentally different from conventional approaches. It does not rely on high-speed electronics and enables transmission of various time multiplexed analog waveforms or digital data signals with the maximum possible symbol rate in the same rectangular optical spectral band B . The aggregate symbol rate of N signal channels corresponds to B or twice the used modulator's electro-optical bandwidth. By a modification of the system, it can be increased to three times the modulator bandwidth. The rectangular spectra can be further multiplexed into wavelength-superchannels without guardbands. To time demultiplex single signal channel, just another intensity modulator and a detector with an electrical bandwidth corresponding to the channel's baseband width ($B/(2N)$) is required. No optical filter, high-speed signal processing, or unconventional photonic devices are needed; thus, it has the potential to be easily integrated into any platform and provides an economical and energy-efficient solution for future communication networks and microwave photonic links.

© 2021 Optical Society of America under the terms of the [OSA Open Access Publishing Agreement](#)

1. Introduction

According to Cisco's annual internet report [1], 66% of the eight billion-world population in 2023 will be connected to the internet. An unforeseeable worldwide crisis can push the growth rates even further and much faster. For example, the Covid-19 pandemic and the implementation of confinement measures have increased the Internet traffic demands up 20% almost within a week. Applications for remote working and education, including VPN and video conferencing, have seen traffic increases beyond 200%, shifting the entire business traffic from the business districts into residential areas [2]. To fulfill such data demands and improve the overall productivity and efficiency of the economy in normal circumstances, maximization of the bandwidth and capacity of intra-datacenter communications [3], and backbone and access networks are required. For data centers, data rates of 400 Gbit/s and 1.6 Tbit/s will become necessary in the near future [4] and in 2023, 77% of the internet connections will be based on mobile devices [1]. For large cell sites in wireless access networks like 5G, an aggregate data rate of up to 100 Gbit/s is required [5]. Especially in data centers and access networks with many interconnects, costs and energy consumption play a vital role in incorporating future standards.

Today, transmission networks predominantly rely on massive high bandwidth electronic digital signal processing (DSP). High sampling rate analog to digital converters (ADCs) in the transmitters and digital to analog converters (DACs) in the receivers are inevitable in conventional optical links [6]. Additionally, for wireless access over fibers, diverse digital radio frequency (RF) signals have to be transferred into the optical domain and vice versa by high bandwidth electronics. The required bandwidth of the electronic signal processors and their energy consumption increases with increasing data rates [7], and the large-scale integration of high-bandwidth modulators on a cost-effective platform like silicon-on-insulator is still quite challenging.

This article presents a new signal transmission method that enables the transmission of analog waveforms and digital data with the maximum possible symbol rate in a rectangular spectral band, without any error. The technique is fundamentally different from other maximum possible symbol rate transmission methods like Nyquist wavelength division multiplexing (N-WDM), orthogonal frequency division multiplexing (OFDM), or any of their derivatives and does not rely on high-speed electronic ADC, DAC, DSP, or unconventional photonic components.

As long as the Nyquist-Shannon sampling theorem limit [8] is not violated, different analog or digital input signals of different modulation formats and versatile spectral width will be multiplexed, transmitted, and individually demultiplexed without any loss in information.

In the transmitter, just a single modulator and a radio frequency network based on a mixer or a frequency multiplier and a phase shifter are required to sample and multiplex N channels in the time domain into an optical rectangular spectral band of width B . If the bandwidth of digital signals is adapted to the channel by an electrical filter, like a raised cosine one, for instance, the N channels' aggregate symbol rate corresponds to twice the electro-optic (E/O) bandwidth of the modulator $B = 2B_M$. This results in the maximum possible symbol rate transmittable in this bandwidth. The rectangular channels multiplexed in time-domain can be further multiplexed into wavelength division super-channels without any guard band. The method is very robust against a jitter of the time or drift in wavelength domain channels.

In the receiver, to demultiplex the single signal channel from the wavelength-superchannel, no optical filter or high-bandwidth electrical sampling is required. Just a single intensity modulator along with a low-bandwidth coherent detector is sufficient. The required bandwidth of the modulator and the detector is just that of the single signal channel $B/(2N)$.

As a proof of concept, we have experimentally demonstrated for the first time in our knowledge that, different kinds of time multiplexed analog waveforms and digital data signals of versatile complex modulation formats occupying the same rectangular spectral band, can be transmitted, time demultiplexed, and received error-free with low bandwidth standard telecommunication devices at a theoretically maximum spectral efficiency. A complete mathematical description behind the concept is also provided.

Due to its simplicity and the possibility to achieve high data rates with low bandwidth electronics and photonics and without massive signal processing, full integration into any electronics-photonics platform is straightforward. Thus, this proposed agnostic transceiver will provide a way to keep pace with the increasing demand and complexity of tomorrow's communication networks. As it can transmit and receive any signal waveform within a specific theoretically defined bandwidth, it will also be beneficial to the microwave photonics links.

2. Principle of operation

The operation principle of the agnostic sampling transceiver (AST) can be seen in Fig. 1. The basic idea of the AST is to use orthogonal sinc sequences for the sampling, multiplexing, and demultiplexing of N signal channels. Sampling and multiplexing can be carried out in only one modulator for all channels with the radio frequency network (RF-NW, green dashed box) shown in Fig. 1. For complex modulation formats, an I-Q modulator and for intensity modulation, a corresponding intensity modulator is required in the transmitter.

The main difference of the AST compared to all other transmission methods lies in the fact that here instead of the signal itself only the sampling points of the signals are multiplexed and transmitted. Thus, the signal has to be sampled first, and as long as the sampling theorem is not violated, the transmitter is entirely agnostic to the input signal. It can be any digital or analog one, and the signal can have any bandwidth up to half the sampling rate.

In the first step, the AST samples all N input signals s_0, s_1, \dots, s_{N-1} with sinc sequences with $N - 1$ zero crossings between two consecutive pulses in the sequence [9–11]. Consequently, the sinc sequences are weighted with the input signals giving the sampling points $C_{0,k}, C_{1,k}, \dots$

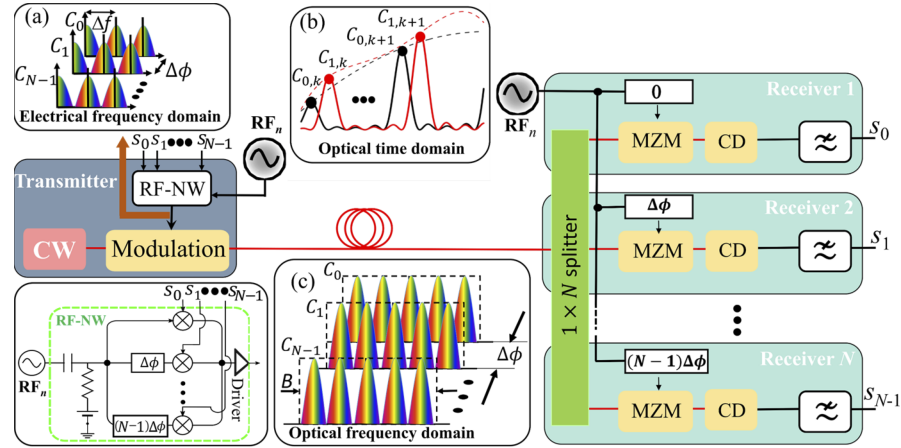


Fig. 1. Schematic representation of the agnostic sampling transceiver system. In the transmitter (left), N channels will be sampled, multiplexed, and transferred to the optical domain by one single modulator (Modulation). The modulator must be suitable for the required modulation format. The optical wave is generated by a laser diode (Laser) and the N signals are pre-processed by a radio frequency network (RF-NW), consisting of electrical mixers or multipliers and phase shifters. The RF-NW is driven with n sinusoidal radio frequencies, generated by a generator (RF_n). The electrical signal after the RF-NW for $n = 2$ sinusoidal frequencies with a spacing of Δf , leading to $N = 2n + 1 = 5$ sampled signal channels in the modulator is shown in inset (a). Due to the phase shift between the sinusoidal frequencies, all these N channels (C_0, C_1, \dots) can be multiplexed into the same rectangular optical bandwidth $B = N\Delta f$ (c). In the time domain (b), this corresponds to the orthogonal multiplexing of the sinc-sequences, weighted with the sampling points of the N input channels ($C_{0,k}, C_{1,k}, \dots$). In the frequency domain (c), the different signal channels have a phase shift of $\Delta\phi = 2\pi/N$ to each other. In the N receivers (right), the signals are demultiplexed in a single intensity modulator like a Mach Zehnder (MZM) and transferred back to the electrical domain by a coherent detector (CD). If the detector's electrical bandwidth is higher than $B/(2N)$, an electrical low pass filter is required at the output.

as shown in Fig. 1(b). Due to orthogonality and corresponding zero-inter-symbol-interference (zero-ISI) between the sequences [12], the N different channels containing the sampling points can be multiplexed in the time domain.

If one intensity modulator is driven with n sinusoidal RF waves with the frequency spacing Δf , the bias and RF power can be adjusted in a way, that at the optical output of the modulator $N = 2n + 1$ lines with equal amplitudes and phases are present [13]. This N -line frequency comb with the bandwidth $B = N \times \Delta f$ corresponds to a sinc sequence in the equivalent time-domain. Mathematically, a sinc sequence is the superposition of ideal sinc-pulses time shifted by $1/\Delta f$. Two of these sinc pulses are orthogonal to each other if they have a time shift of m/B to each other, with $m = 1, 2, \dots, N - 1$ [12]. Thus, the sinc sequence generated by the modulator can be split into N parallel channels, time-shifted by m/B for the m -th channel, and multiplied with the N signals with N intensity modulators, resulting in a sampling of each signal [9–11]. Afterward, these N channels can be summed up to build the multiplexed time-domain channel [12].

However, the same result can be achieved if just one modulator is used and the electrical current applied to the modulator is the signal itself, plus the signal electrically multiplied with the sinusoidal frequencies. The electrical spectrum for the different channels C_0, C_1, \dots, C_{N-1} ,

is shown in inset (a) of Fig. 1 for $n = 2$, leading to $N = 5$ signal channels. Between adjacent pulses in the sequence, there are $N - 1$ zero-crossings. Thus, N signal channels, time-shifted by $1/B$ would be orthogonal to each other. In the equivalent frequency domain, a time shift is a phase change. Hence, all the N independent signal channels can be processed in an electrical network, if the sinusoidal frequencies are phase-shifted by $\Delta\phi = 2\pi/N$. These N signals can be added together and used to drive one single modulator for the sampling and multiplexing of the N channels (see inset (a) in Fig. 1 for the electrical spectrum of the N signal channels after the RF-NW). Consequently, in the RF network (green dashed box in Fig. 1), a bias tee, a phase shifter, and an electrical multiplier for each signal channel are required. If an electrical mixer is used instead of the multiplier, the baseband signal must be bypassed to keep it in the spectrum.

Due to the bias adjustment of the modulator with the bias tee, the electrical spectrum is mirrored around the optical carrier with equal phase and amplitude [9] (Fig. 1(c)). For the single channel, this corresponds to a convolution of the signal spectrum with an N -line frequency comb, leading to N copies of the signal spectrum. In the equivalent time domain, this convolution is the multiplication of the signal with a sinc sequence or the sampling of the signal [9–11]. Due to the phase shift between the frequency combs and the corresponding orthogonality, this is independently done for all N signals in one single modulator (see inset (b) in Fig. 1 for the time and (c) for the frequency domain representation of the sampled and multiplexed signals).

In the receiver, the orthogonality of the sinc sequences is exploited to demultiplex the single channel in another single modulator [14]. Here independent of the modulation formats, a single intensity modulator is sufficient. The multiplexed input signal has to be divided into N copies for the N receivers. The input signal power for each receiver is divided by N as well. The modulator in each receiver multiplies the received multiplexed input with a sinc sequence with the right time shift. This can be simply achieved by driving the modulator with the same sinusoidal frequencies and adjusting the bias and RF power [9]. The channel to be demultiplexed is determined by the phase shift of the sinusoidal signal. Thus, synchronization between the sinusoidal frequencies in the transmitter and receiver is required. This can be achieved by simply scanning the radio waves in the receiver over a phase shift of 2π and then locking the phase shift to the maximum eye-opening of the output signal. As we will show in the results section, slight changes of the phase do not severely degrade the transmission. Since all N channels will have a maximum eye-opening, information about the channel number has to be transmitted for the first adjustment after an interruption of the connection.

The original signal s_0, s_1, \dots, s_{N-1} is retrieved from the sampling points after detection with a coherent detector (CD). If the detector bandwidth is higher than that of the single channel in the baseband $B/(2N)$, electrical low-pass filtering is required. A more comprehensive discussion on the functionalities of the various segments is included in [Supplement 1](#). There it is shown by a mathematical proof that, for ideal and noiseless components the AST samples, multiplexes, transmits, and demultiplexes the data without any loss in information.

For the sampling, the signal bandwidth is limited by the Nyquist-Shannon sampling theorem. Thus, the sampling rate for the signal in the single channel has to be twice the maximum baseband bandwidth of the signal. If a data signal is spectrally limited by an electrical filter to half of the sampling rate, the aggregated symbol rate can be twice the E/O bandwidth of the modulator and the bandwidth of the rectangular optical spectrum corresponds to the symbol rate. Thus, like orthogonal frequency division multiplexing (OFDM) and Nyquist-wavelength division multiplexing (N-WDM), the method enables the transmission with the maximum possible symbol rate. However, in complete contrast to these two methods, no complex and high-bandwidth optical, electrical, or electronic signal processing is required. The signal is sampled and multiplexed with sinc sequences in the optical modulator. Thus, for the electrical filtering to achieve the maximum possible symbol rate, a raised cosine or similar filter with a roll-off factor of 0.1, easily achievable as an electronic or digital one, is sufficient.

All the N signal channels are time-domain multiplexed (TDM) into the same rectangular spectrum of bandwidth B . Several such rectangular bandwidth channels can be further multiplexed in the frequency domain to form a wavelength division – time-division (WDM-TDM) superchannel. For the demultiplexing of these WDM-TDM superchannels in the single receiver, no additional equipment and especially no optical filter are required. In the receiver, the WDM channel is defined by the local oscillator's center wavelength in the coherent detector and the TDM channel by the phase shift of the electrical sinusoidal waves. Since the bandwidth is rectangular and no optical filter is needed, no guard band between the channels is required. Thus, in a channel with a bandwidth B_c the transmittable symbol rate corresponds to this bandwidth and is equal to the theoretically maximum symbol rate of this channel.

Especially in the receiver, low bandwidth equipment is sufficient for retrieving the signal. A reduction of the signal processing bandwidth results in less energy consumption, and the simplicity of the technique enables integration into any platform suitable for mass production. Therefore, this method will be especially interesting in fields where high bandwidth signals have to be delivered with high energy efficiency at low costs, such as 5G, 6G, and data centers. The most basic operation i.e. sinc sequence generation and sampling has already been demonstrated in the cost effective silicon photonics platform [15,16]. Since all parameters for the agnostic transceiver can be promptly and simply defined in the electrical domain, the receiver and detector can be adapted to the channel requirements during the transmission. Thus, the agnostic sampling transceiver will be ideal for elastic optical networks [17,18].

3. Results

To experimentally demonstrate the underlying concept of the agnostic sampling transceiver, we adopted a proof of concept experimental setup with off-the-shelf telecom equipment similar to that shown in Fig. 1 (see Supplement 1 for a detailed description). Since the RF equipment was not available for the proof of concept setup, it was mimicked by Matlab code and an arbitrary waveform generator (AWG). This AWG, however, has limited all single carrier experiments to an aggregated bitrate of 48 Gbit/s. Polarization diversity was not implemented and only one receiver was used to reduce complexity. In this single receiver, the different channels were demultiplexed successively. The data signal transmission experiments were carried out for more than 300,000 bits. We did not use any nonlinearity or chromatic dispersion compensation, and forward error correction was not implemented.

In the first experiments, only one carrier wavelength was implemented and the number of signal channels was $N = 3$. Thus, we had one TDM channel consisting of three independent signal channels. The three input signals were multiplied with an amplitude-shifted 8 GHz sinusoidal signal with three different phase shifts of 0° , 120° , and 240° before applying to the modulator. To show the agnostic behavior of the sampling transceiver, for the first experiment in one signal channel BPSK data (a), in another a PAM4 signal (b), and in the third, a sinusoidal signal (c) was sampled, multiplexed, transmitted, and demultiplexed, as shown in Fig. 2. A Mach-Zehnder Modulator was used in this case at the transmitter as well as receiver. The digital data was transmitted without any bit error, and the analog sinusoidal signal shows almost no distortion.

For the following experiments, we have replaced the MZM in the transmitter with an I-Q modulator. The in-phase (I) and Quadrature (Q) components were processed separately in the same way as described for the single modulator before feeding into the I and Q branch of the modulator. As described in the previous section, an intensity modulator is sufficient for demultiplexing I-Q modulated signals. Thus, in the receiver, nothing has been changed.

First, we have investigated the processing and transmission of three 4 GBd 16 QAM signal channels with a pseudo-random bit sequence ($2^9 - 1$). The data channels were again multiplied with phase-shifted 8 GHz sinusoidal signals and applied to the I and Q branch of the modulator.

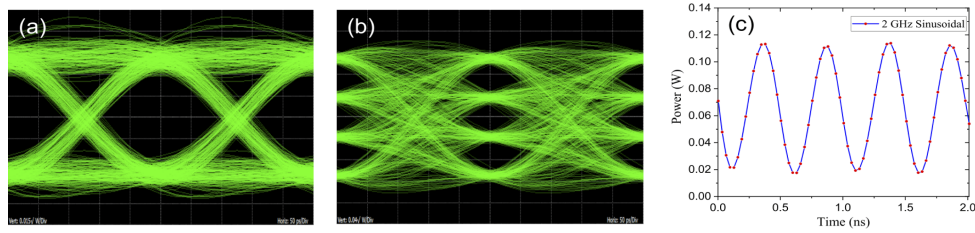


Fig. 2. Received signals after 10 km of fiber for three different signal channels modulated with the AST on a single carrier. The channels were modulated with a 4 GBd BPSK (a), a 4 GBd PAM4 (b) and a 2 GHz sinusoidal signal (c).

The measured signal constellation diagrams are presented in Figs. 3(a), (b), and (c) for a back-to-back (B2B) transmission, a 10 km and a 30 km single-mode fiber transmission, respectively. The aggregated symbol rate is 12 GBd, corresponding to an aggregated data rate of 48 Gbit/s whereas, the baseband bandwidth is 12 GHz and the optical rectangular channel bandwidth is 24 GHz. Since the single channel with an electrical bandwidth of 4 GHz is multiplied with the 8 GHz sinusoidal wave, the Nyquist-Shannon sampling theorem is fulfilled [8]. Thus, the data is transmitted without any bit error, as evident from the error vector magnitude (EVM), Q-factor, and bit error rate (BER) measurements for the 16-QAM signals. The EVM as a percentage is the root mean square (rms) average distance of the received symbol to the ideal one. The Q-factors were measured following the decision threshold method [19].

The maximum possible symbol rate, which can be transmitted in a channel with the optical bandwidth B_c is equal to this bandwidth. The AST has to follow the sampling theorem, so, to double the symbol rate compared to the previous experiments, we have filtered the data to the Nyquist limit. With a raised cosine filter with 0.1 roll-off factor, the 8 GBd QPSK signal was restricted to 4 GHz baseband width. Consequently, as for OFDM and N-WDM, the agnostic transceiver can transmit data with the theoretically maximum symbol rate, transmitting 24 GBd in a rectangular optical bandwidth of 24 GHz. Note that a roll-off factor of 0.1 is far away from a rectangular shape and easily achievable with microwave or digital filters. The rectangular shape of the TDM channel results from the sinc sequences transmitting the sampling points of the signal. In Figs. 3(d), (e), and (f), the measured signal constellation diagrams are shown for different transmission ranges for 8 GBd QPSK signals. Similar to the previous case, three channels were transmitted together, while each channel was demultiplexed successively. We have also transmitted 3×4 GBd 16 QAM signals by the sampling transceiver in a 12 GHz optical bandwidth. The constellation after 10 km of SMF transmission is shown in Fig. 3(g). For all the cases the aggregated bitrate is 48 Gbit/s, restricted by our equipment.

Figure 3(h) depicts the EVM and Q factor variation with the optical signal to noise ratio (OSNR). The measurement of the OSNR sensitivity was carried out by varying the amount of attenuation with a variable optical attenuator (VOA) at the transmitter's output, i.e. after the modulator (see Fig. S4 in Supplement 1). For these measurements, a 4 GBd 16 QAM and 8 GBd QPSK were sampled with an 8 GHz sinusoidal wave in the sampling transceiver, i.e. 12 GBd in a channel bandwidth of 24 GHz for the 16-QAM and 24 GBd in 24 GHz for the QPSK.

One of the major advantages of the AST is, that the channels are transmitted in a rectangular spectral band. Thus, the N signal channels building a TDM channel can be further multiplexed in the wavelength domain to construct a WDM-TDM superchannel. The achievable spectral efficiency in an ultra-dense wavelength division multiplexed system depends on how close the individual carriers can be placed. We investigated the performance of the agnostic transceiver in terms of the inter-channel overlap as presented in Fig. 4. The carrier spacing between three independent single carrier TDM channels with maximum symbol rate and a bandwidth of 24

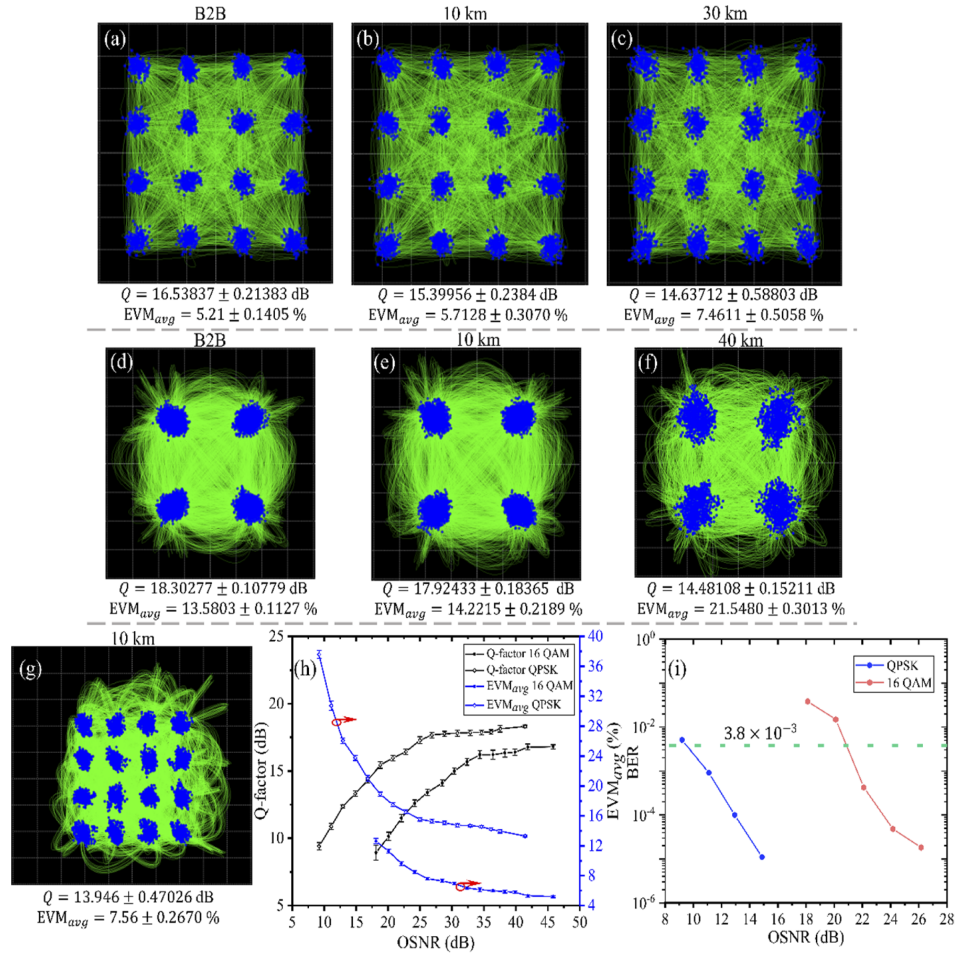


Fig. 3. Single carrier agnostic sampling transceiver performance. Measured constellation diagrams, Q-factors, and average EVM values for sinc-sequence demultiplexed 4 GBd 16 QAM signals with 4 GHz baseband width after different fiber transmission distances (a-c). B2B denotes back-to-back, where the transmitter is directly connected to the receiver. The corresponding average error vector magnitudes (EVMs) and Q-factors (Q) are also given. If 8 GBd QPSK signals are filtered down to 4 GHz of baseband width by a raised cosine filter with a roll-off factor of 0.1, the signal constellations after different fiber lengths are shown in (d-f). For (a-f) the optical channel bandwidth was 24 GHz, while the aggregated symbol rate was 12 GBd for (a-c) and 24 GBd for (d-f), corresponding to the maximum symbol rate. In (g) one of three 4 GBd—16 QAM signal channels multiplexed into a 12 GHz optical bandwidth after 10 km of fiber is presented. Since the aggregated symbol rate is again 12 GBd, this corresponds to the maximum symbol rate. Q-factor, average EVM, and BER performances in terms of OSNR are shown in (h) and (i). The 16 QAM measurements correspond to (a-c) and the QPSK measurements to (d-f). No digital chromatic dispersion compensation, nonlinearity compensation, or forward error correction was considered in encoding or analyzing the data. In (i) the hard decision FEC limit (3.8×10^{-3}) is marked with a green dashed line.

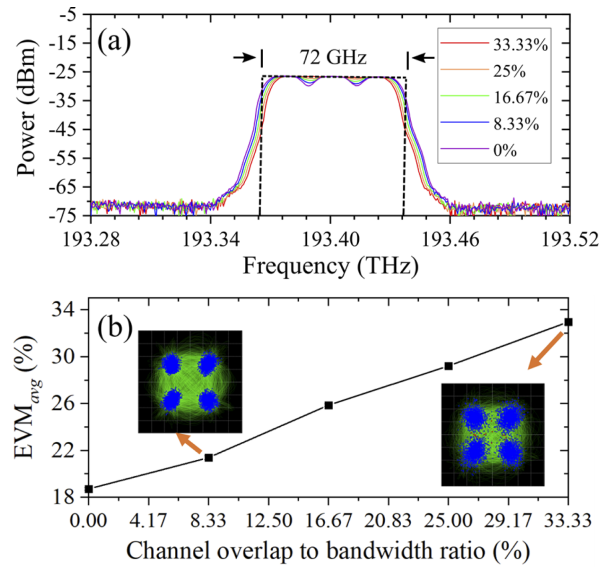


Fig. 4. EVM penalty in terms of channel overlap. If three different TDM channels (each carrying three signal channels) with different carrier frequencies are multiplexed to a WDM superchannel, the resultant spectra after multiplexing having a different spacing between the spectral channels are shown in (a). The dashed box shows the rectangular bandwidth for $3 \times 24 \text{ GHz} = 72 \text{ GHz}$. The spectrum measurements were carried out with an optical spectrum analyzer at 10 GHz resolution. The channel overlap is given relative to the bandwidth of the single TDM channel. Thus, an overlap of 33.3% means that only 2/3 of the channel in the middle are free from interference from neighboring channels, 1/6 is overlapped by the left and another 1/6 by the right channel. The EVM performance with varying spectral spacing to assess the potential spectral efficiency is presented in (b). The insets show the measured constellation diagrams for the corresponding channel overlap.

GHz was varied from 24 GHz (corresponding to no guardband, or 0% spectral overlap) to 20 GHz (corresponding to -4 GHz guardband or approximately 33.33% spectral overlap). At 20 GHz spacing, only two-third of the channel in the middle are free from the overlap by neighboring channels. The middle channel was modulated with an 8 GBd filtered QPSK signal, while the adjacent channels were modulated with 8 GBd filtered BPSK signals. This ensures uncorrelated data streams at the receiver. If the channels overlap, the EVM increases as expected. However, the BER of the signal channels remains below the FEC limit until one-third of the channel bandwidth is overlapped by the adjacent channels. This shows that the TDM channels can be multiplexed to robust WDM superchannels without any guardband and virtually without any loss in information. Additionally, in contrast to OFDM and N-WDM even quite high frequency drifts between the sub-channels only slightly influence the signal transmission. The same holds for a jitter of the radio frequency driving the modulator in the transmitter or receiver for the multiplexing and demultiplexing of the signals. We have simulated the influence of the jitter showing only a limited response till a jitter ratio of 7%, which equals 8.75 ps for the 8 GHz sine wave. Until this value, the BER is below the FEC limit. State of the art RF sources show jitter values in the range of femtoseconds, e.g. the Keysight E8257D with 22 fs at 10 GHz [20] or the VCO HMC732 from Analog Devices with 140 fs at 8 GHz [21]. This shows as well that the transmission is quite robust against a slight phase change of the sine waves driving the transmitter and receiver modulators.

Using one laser and a 5-line optical comb generated from a phase modulator we transmitted a superchannel consisting of 5×3 QPSK signal channels with no guardband between the channels at a line rate of 240 Gbit/s in a 120 GHz optical bandwidth. Moreover, using three lasers and subsequent phase modulation to get nine comb lines, we could achieve a line rate of 432 Gbit/s for 9×3 QPSK signal channels within an optical bandwidth of 216 GHz. For all these experiments we have demultiplexed the signal channel in the middle of the spectrum and no bit error was measured for 300,000 transmitted bits.

4. Comparison with existing orthogonal multiplexing methods

To transmit signals in a limited bandwidth with the maximum possible symbol rate particularly two methods, i.e. OFDM and N-WDM with many derivatives have been established in the last few years. Sinc sequences are the ISI-free superposition of time-shifted single sinc-pulses [12]. Therefore, OFDM and N-WDM's commonality with the AST is that the orthogonality of sinc pulses is exploited to multiplex the signal channels independently. Additionally, all three methods enable signal transmission with the maximum possible symbol rate. In contrast to our method, however, OFDM and N-WDM need either high-bandwidth and energy inefficient electronics or unconventional photonic components for signal processing.

For OFDM the channels are orthogonal in the frequency domain, i.e. orthogonal sinc-shaped sub-carrier spectra extend into adjacent frequency slots and the time symbols are rectangularly shaped. For N-WDM the orthogonality of sinc-shaped time symbols is exploited. The symbols extend into adjacent time slots, and the spectra of the sub-channels are rectangular. The channel spacing for N-WDM is equal to the symbol rate.

Figure 5 shows the fundamental differences between OFDM, N-WDM, and the sampling transceiver proposed here in the time (top) and frequency domain (bottom). For ideal OFDM (Fig. 5(a)) the rectangular symbol with a time duration T_S has a frequency representation of an ideal sinc shaped spectrum with a spectral width of $\Delta f = 1/T_S$ from the center to the first zero-crossing. By exploiting the orthogonality (or the zero-ISI) between the sinc shaped spectra, the subsequent sub-carrier frequency has to be in the zero-crossing of the previous one. Thus, the next rectangular time symbol is directly adjacent to the previous.

OFDM signals overlap in the spectrum, their generation and demultiplexing can be achieved by an inverse or forward Fourier transform of all channels together in a digital signal processor (DSP). However, for high symbol rates, this requires very high bandwidth electronics for the transmitter and receiver. Alternatively, N single independent laser sources and N modulators can be used to generate N sub-channels [22]. This requires a precise frequency locking between the independent sources. Otherwise, the orthogonality between the channels will be lost. Additionally, if the N modulators required for the sub-channels do not have a bandwidth that exceeds the combined bandwidth of all the sub-carriers together, the phase and amplitude in each sub-carrier will vary, leading to a loss of orthogonality at the receiver [23]. For high bandwidth transmission, optical methods can be used for the multiplexing and demultiplexing of OFDM signals. In the optical domain, the forward or inverse Fourier transform can be achieved with banks of optical filters or arrayed grating wavelength routers [23]. However, this requires unconventional optical components and a tuning mechanism for flexible bandwidth allocation is challenging.

N-WDM (Fig. 5(b)) follows the same concept as OFDM but with the time and frequency domain inverted. For ideal N-WDM the symbol in the time domain is a sinc-pulse. Thus, to exploit the zero-ISI between the sinc-pulses, the next symbol can be at the zero-crossing of the previous and the bandwidth of the single WDM channel is $B = 1/T_S$. Due to the rectangular shape of the spectral channel, the next N-WDM channel can be directly adjacent to the previous without any guard band in between. For N-WDM, a rectangular spectrum is desired to multiplex each single WDM channel. A perfect rectangular spectrum requires an infinitely long sinc-pulse, which is impossible in practice. Thus, in many N-WDM experiments, high-bandwidth electronic

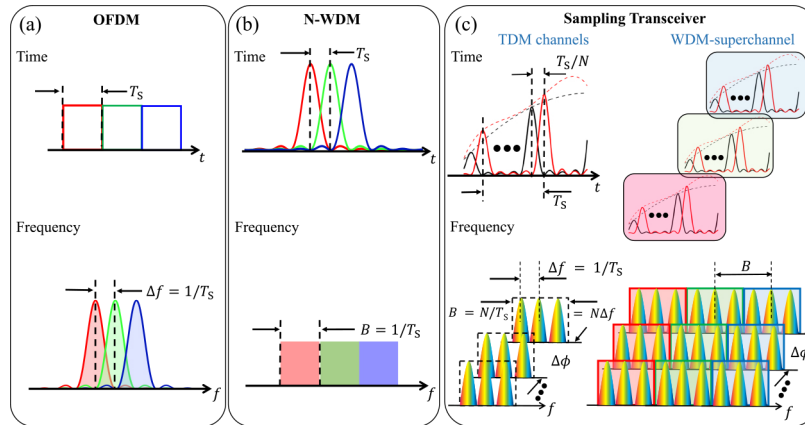


Fig. 5. Comparison between OFDM (a), N-WDM (b), and the agnostic sampling transceiver (c) in the time (top) and frequency domain (bottom). OFDM and N-WDM use single sinc-shaped signals in the frequency (OFDM) or time-domain (N-WDM) to multiplex several sub-channels. OFDM and N-WDM sub-channels orthogonally overlap in the frequency or time domain, respectively. For the agnostic sampling transceiver (c) not discrete sinc pulses but periodic sinc-sequences are used (top), which results in N time-domain signal channels forming one TDM channel inside the same rectangular spectral band (bottom left in (c)). In the bandwidth $B = N\Delta f$ all the N channels have a different phase shift of $\Delta\phi = 2\pi/N$ to each other. Several such TDM channels can be multiplexed to form WDM-TDM superchannels without any guardband (bottom right in (c)) and with flexible bandwidth allocation.

signal processing has been used to shape the pulses as close as possible to single sinc-pulses [24]. This requires digital filters with a large number of filter coefficients or optical or electrical filters with steep edges and specific filter shapes [25]. Another possibility is the rectangular as possible filtering of a frequency comb produced by a mode-locked laser for instance [26], or a so-called Nyquist laser [27]. Filters with infinitely steep edges are not possible in practice. However, filters based on the stimulated Brillouin scattering (SBS), can have very sharp edges with a 250 dB/GHz roll-off [28], but with a limited extinction. Since the orthogonality holds only at the zero crossings of the channels, a high sampling rate receiver is required for the reception of N-WDM signals.

The proposed agnostic sampling transceiver is illustrated in Fig. 5(c). Although like OFDM and N-WDM it exploits the zero-ISI of sinc-pulses, it has several significant differences. First, before multiplexing and transmission, the signal is sampled. Hence, it is not assumed that ideal rectangular time-symbols for OFDM or sinc-pulses as for N-WDM are present. Instead, only the sampling points are transmitted, and the signal to be sampled can be any analog or digital signal with any bandwidth limited by $\Delta f/2$ in the baseband. If a digital signal is restricted in its baseband bandwidth to $\Delta f/2$, the aggregated symbol rate in all N channels is the same as for OFDM or N-WDM. It thus corresponds to the maximum achievable symbol rate. Note that, unlike N-WDM, the filter is not used to shape the signal spectrum, but only to limit it. In the experiments, we have used a raised cosine filter with a roll-off factor of only 0.1.

Another important difference is, that for the sampling, multiplexing, and demultiplexing sinc sequences are used. These sinc sequences are a summation of time-shifted sinc-pulses [12]. In the frequency-domain, the periodic sinc-pulses are represented by a rectangular, phase-locked frequency comb with N tones, separated by $\Delta f = 1/T_s$ having a total bandwidth of $B = N\Delta f = N/T_s$. Thus, in contrast to N-WDM, not the symbol rate of the single channel, but the aggregated one in all N channels together is the rectangular optical bandwidth B . Since the

sampling theorem is not violated by the sampling transceiver, the spectral components do not overlap. Thus, in contrast to OFDM, the spectra do not extend into adjacent frequency slots. Additionally, in contrast to OFDM, the single frequencies of the rectangular comb do not define the TDM sub-channels. In contrast to N-WDM, the symbol duration for the single sub-channel does not correspond to the inverse bandwidth of the pulses.

The sinc sequence has $N - 1$ zero crossings. Therefore, in the time domain, N signal channels can be multiplexed together with zero-ISI to form one TDM channel, if the next signal channel is in the zero-crossing of the previous one, satisfying orthogonality. In the frequency domain, the time shift is a linear phase change. Thus, each of these N signal channels spreads over the same bandwidth B , having a phase shift of $\Delta\phi = 2\pi/N$ to each other (bottom left inset in Fig. 5(c)). Due to the rectangular bandwidth, several such TDM channels can form a WDM-TDM superchannel, (bottom right inset in Fig. 5(c)). Since the spectra do not extend into adjacent frequency slots, and since no optical filter is used to separate the channels, the next WDM channel can be directly adjacent to the previous one, without any guard band in between. Therefore, the carrier frequency difference between the two channels can correspond to the comb or TDM channel bandwidth B . Even a slight overlap of the channels does not severely degrade the performance of the transmission. Thus, in contrast to OFDM and N-WDM, the AST is very robust against a frequency drift between the wavelength channels. Since the WDM-TDM channels can have flexible bandwidth allocations, the method offers the possibility to adapt the modulation and multiplexing to the requirements of every single channel and this adaptation can be done by the electrical signal driving the modulator.

5. Transmittable symbol rate

If the sinc-pulse generation and multiplexing of all N channels are carried out with only one modulator of E/O bandwidth B_M , the maximum bandwidth of the generated optical frequency comb convoluted with the signal spectrum corresponds to $2B_M$. In this case, the maximum symbol rate for one channel can be $B_B = 2B_M/N$. Thus, the aggregated symbol rate of all N channels together corresponds to twice the bandwidth of the modulator $2B_M$. The symbol rate can be increased if the pulse generation and sampling are carried out in two consecutive modulators. If one single modulator is driven with n equidistant sinusoidal radio frequencies for pulse generation, the modulator generates a rectangular frequency comb with $N = 2n + 1$ lines in the optical domain. In this case, the maximum bandwidth of the comb convoluted with the signal spectrum corresponds to $2N/(N - 1)B_M$, with B_M as its maximum RF bandwidth, or $3B_M$ for $N = 3$ and $n = 1$. Thus, the aggregated symbol rate in all three channels together would be $3B_M$.

6. Conclusion

In conclusion, we have presented and experimentally demonstrated a new kind of transceiver concept, which is entirely agnostic for the signals to be transmitted (bandwidth up to $\Delta f/2$, complex modulation, analog or digital) and allows the data transmission with the maximum possible symbol rate. In only one single modulator, the signals of N different electrical inputs, which can be intensity or phase-modulated digital or analog ones, are optically sampled with sinc sequences and time-division multiplexed to build a TDM channel with a rectangular bandwidth. These TDM channels can be further multiplexed to form WDM-superchannels without any guardband. With one integrated modulator with an E/O bandwidth of 500 GHz [29] and only one wavelength, N multiplexed signals with an overall symbol rate of 1 TBd can be multiplexed and transmitted in a rectangular optical bandwidth of $B = 1$ THz. With a modulator for pulse generation and one for sampling, the symbol rate (and optical bandwidth) could increase to 1.5 TBd. This can easily be enhanced by increasing the number of carriers. For the receiver a modulator and detector with the baseband bandwidth of the single channel $B/(2N)$ are sufficient. No optical delay lines, filters, phase shifters, or broadband digital signal processing is required.

The mathematical description indicates that the concept can be generalized to any carrier frequency. Due to the simplicity of the method, integration into silicon photonics or any other equivalent platform is straightforward, enabling cost-effective mass production. Thus, the method will be especially interesting for applications like access and wireless networks, microwave photonic links, and data centers where various types of signals have to be transmitted at once.

Funding. Deutsche Forschungsgemeinschaft (DFG, German Research Foundation) (322402243, 403154102, 424608109, 424608271, 424607946, 424608191); German Federal Ministry of Education and Research (BMBF, Bundesministerium für Bildung und Forschung) (13N14879).

Acknowledgments. We thank Younus Mandalawi and Dr. Ranjan Das from TU Braunschweig for the constructive discussions.

Disclosures. The authors declare no conflicts of interest.

Data Availability. Data may be available from the corresponding author upon reasonable request.

Supplemental document. See [Supplement 1](#) for supporting content.

References

1. Cisco Annual Internet Report (2018–2023) White Paper [Online]. (2020).
2. A. Feldmann, O. Gasser, F. Lichtblau, E. Pujol, I. Poese, C. Dietzel, D. Wagner, M. Wichtlhuber, J. Tapiador, N. Vallina-Rodriguez, O. Hohlfeld, and G. Smaragdakis, “The Lockdown Effect: Implications of the COVID-19 Pandemic on Internet Traffic,” in *Proceedings of the ACM Internet Measurement Conference* (ACM, 2020), pp. 1–18.
3. C. L. Schow and K. Schmidtke, “INTREPID: Developing Power Efficient Analog Coherent Interconnects to Transform Data Center Networks,” in *Optical Fiber Communication Conference (OFC) 2019* (OSA, 2019), p. M4D.9.
4. J. Verbist, M. Vanhoecke, M. Lillieholm, S. A. Srinivasan, P. De Heyn, J. Van Campenhout, M. Galili, L. K. Oxenlowe, X. Yin, J. Bauwelinck, and G. Roelkens, “4:1 Silicon Photonic Serializer for Data Center Interconnects Demonstrating 104 Gbaud OOK and PAM4 Transmission,” *J. Lightwave Technol.* **37**(5), 1498–1503 (2019).
5. J. Shihuan Zou, S. Adrian Sasu, M. Lawin, A. Dochhan, J.-P. Elbers, and M. Eiselt, “Advanced optical access technologies for next-generation (5G) mobile networks [Invited],” *J. Opt. Commun. Netw.* **12**(10), D86–D98 (2020).
6. “Implementation Agreement for Integrated Dual Polarization Intradyne Coherent Receivers [online],” https://www.oiforum.com/wp-content/uploads/2019/01/OIF_DPC_RX-01.2.pdf.
7. J. Baliga, R. Ayre, K. Hinton, W. V. Sorin, and R. S. Tucker, “Energy Consumption in Optical IP Networks,” *J. Lightwave Technol.* **27**(13), 2391–2403 (2009).
8. A. V. Oppenheim, A. S. Willsky, and S. Hamid, *Signals and Systems*, 2nd ed. (Prentice Hall PTR, 1996).
9. S. Preußler, G. Raoof Mehrpoor, and T. Schneider, “Frequency-time coherence for all-optical sampling without optical pulse source,” *Sci. Rep.* **6**(1), 34500 (2016).
10. J. Meier, A. Misra, S. Preusler, and T. Schneider, “Orthogonal Full-Field Optical Sampling,” *IEEE Photonics J.* **11**(2), 1–9 (2019).
11. A. Misra, S. Preußler, L. Zhou, and T. Schneider, “Nonlinearity- and dispersion- less integrated optical time magnifier based on a high-Q SiN microring resonator,” *Sci. Rep.* **9**(1), 14277 (2019).
12. M. A. Soto, M. Alem, M. Amin Shoaie, A. Vedadi, C.-S. Brès, L. Thévenaz, and T. Schneider, “Optical sinc-shaped Nyquist pulses of exceptional quality,” *Nat. Commun.* **4**(1), 2898 (2013).
13. M. A. Soto, M. Alem, M. A. Shoaie, A. Vedadi, C.-S. Brès, L. Thévenaz, and T. Schneider, “Generation of Nyquist sinc pulses using intensity modulators,” in *CLEO: 2013* (OSA, 2013), p. CM4G.3.
14. M. A. Shoaie, A. Vedadi, and C.-S. Brès, “A simple all-optical format transparent time and wavelength demultiplexing technique for WDM & orthogonal-TDM Nyquist channels,” in *2015 European Conference on Optical Communication (ECOC)* (IEEE, 2015), pp. 1–3.
15. A. Misra, C. Kress, K. Singh, S. Preußler, J. Christoph Scheytt, and T. Schneider, “Integrated source-free all optical sampling with a sampling rate of up to three times the RF bandwidth of silicon photonic MZM,” *Opt. Express* **27**(21), 29972–29984 (2019).
16. S. Liu, K. Wu, L. Zhou, L. Lu, B. Zhang, G. Zhou, and J. Chen, “Optical Frequency Comb and Nyquist Pulse Generation With Integrated Silicon Modulators,” *IEEE J. Sel. Top. Quantum Electron.* **26**(2), 1–8 (2020).
17. M. Jinno, H. Takara, B. Kozicki, Y. Tsukishima, Y. Sone, and S. Matsuoka, “Spectrum-efficient and scalable elastic optical path network: architecture, benefits, and enabling technologies,” *IEEE Commun. Mag.* **47**(11), 66–73 (2009).
18. M. Jinno, “Elastic Optical Networking: Roles and Benefits in Beyond 100-Gb/s Era,” *J. Lightwave Technol.* **35**(5), 1116–1124 (2017).
19. N. S. Bergano, F. W. Kerfoot, and C. R. Davidson, “Margin measurements in optical amplifier system,” *IEEE Photonics Technol. Lett.* **5**(3), 304–306 (1993).
20. “Datasheet: E8257D PSG Microwave Analog Signal Generator,” Keysight Technol. (2020).
21. “Datasheet: VCO HMC732,” Analog Devices (2021).
22. S. Chandrasekhar and X. Liu, “Experimental investigation on the performance of closely spaced multi-carrier PDM-QPSK with digital coherent detection,” *Opt. Express* **17**(24), 21350–21361 (2009).

23. A. J. Lowery, L. Zhuang, B. Corcoran, C. Zhu, and Y. Xie, "Photonic Circuit Topologies for Optical OFDM and Nyquist WDM," *J. Lightwave Technol.* **35**(4), 781–791 (2017).
24. R. Schmogrow, M. Winter, M. Meyer, D. Hillerkuss, S. Wolf, B. Baeuerle, A. Ludwig, B. Nebendahl, S. Ben-Ezra, J. Meyer, M. Dreschmann, M. Huebner, J. Becker, C. Koos, W. Freude, and J. Leuthold, "Real-time Nyquist pulse generation beyond 100 Gbit/s and its relation to OFDM," *Opt. Express* **20**(1), 317–339 (2012).
25. R. Schmogrow, S. Ben-Ezra, P. C. Schindler, B. Nebendahl, C. Koos, W. Freude, and J. Leuthold, "Pulse-Shaping With Digital, Electrical, and Optical Filters—A Comparison," *J. Lightwave Technol.* **31**(15), 2570–2577 (2013).
26. M. Nakazawa, T. Hirooka, P. Ruan, and P. Guan, "Ultrahigh-speed "orthogonal" TDM transmission with an optical Nyquist pulse train," *Opt. Express* **20**(2), 1129–1140 (2012).
27. M. Nakazawa, M. Yoshida, and T. Hirooka, "The Nyquist laser," *Optica* **1**(1), 15–22 (2014).
28. C. Feng, S. Preussler, and T. Schneider, "Sharp tunable and additional noise-free optical filter based on Brillouin losses," *Photonics Res.* **6**(2), 132–137 (2018).
29. M. Burla, C. Hoessbacher, W. Heni, C. Haffner, Y. Fedoryshyn, D. Werner, T. Watanabe, H. Massler, D. L. Elder, L. R. Dalton, and J. Leuthold, "500 GHz plasmonic Mach-Zehnder modulator enabling sub-THz microwave photonics," *APL Photonics* **4**(5), 056106 (2019).